EXTRACTING STRUCTURAL FEATURES OF RAT SCIATIC NERVE USING MULTI-FUNCTIONAL SPECTRAL-DOMAIN OPTICAL COHERENCE TOMOGRAPHY

MICHAEL C. OLIVEIRA[1], MD. SHAHIDUL ISLAM[1], FRANCIS P. HENRY[2], MARK A. RANDOLPH[2], B. HYLE PARK[1], JOHANNES F. DE BOER[2]

[1]DEPARTMENT OF BIOENGINEERING, UNIVERSITY OF CALIFORNIA, RIVERSIDE, CA 92521

[2]WELLMAN CENTER FOR PHOTOMEDICINE, MASSACHUSETTS GENERAL HOSPITAL, HARVARD MEDICAL SCHOOL, BOSTON, MA 02114

PROJECT SUMMARY

In this study, we used multi-functional spectral-domain optical coherence tomography (OCT) imaging for quantitative characterization of structural and optical features of healthy rat sciatic nerve. Our findings are:

1. Epineurium thickness measurements from OCT and polarization-sensitive OCT (PS-OCT) images agree well with each other as well as previously published measurements.
2. Average birefringence of the sciatic nerve did not change with increasing stretch of the sciatic nerve.
3. The frequency of Fontana's bands is negatively correlated with increasing stretch on the sciatic nerve.
4. Extinction coefficient between sciatic nerve and muscle tissue is different, while birefringence between is not.

MULTI-FUNCTIONAL SPECTRAL-DOMAIN OCT

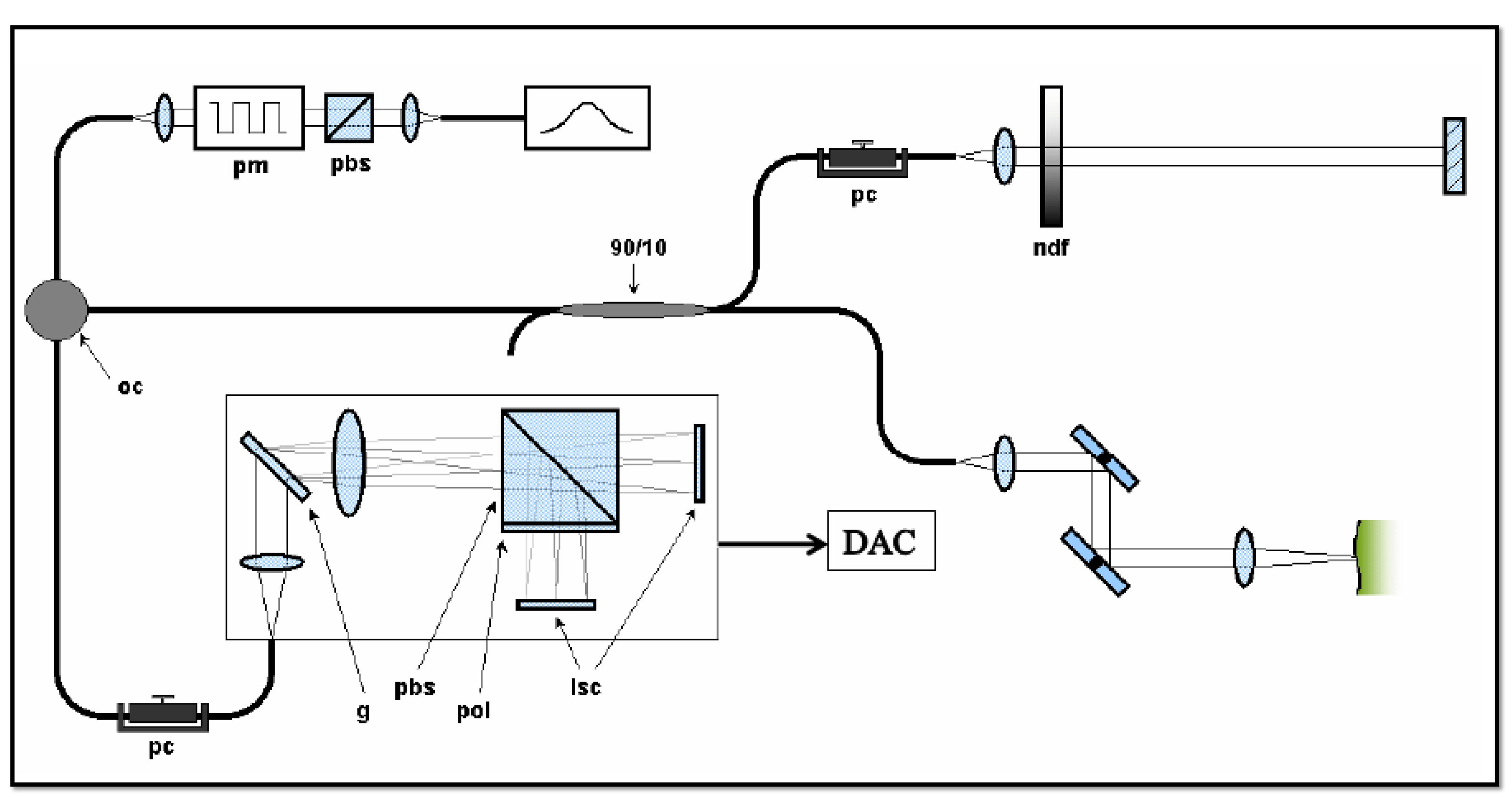

Figure 1. Diagram of the multi-functional 1320 nm SD-OCT system (pbs: polarizing beam splitter, pm: polarization modulator, oc: optical circulator, 90/10: fiber splitter, pc: static polarization controller, ndf: neutral density filter, g: transmission grating, pol: polarizer, lsc: line scan camera), DAC: data acquisition computer.

IMAGING

Raster scanning of the beam was performed on a 5-mm section of the sciatic nerve, perpendicular to the long axis. OCT and PS-OCT images are generated simultaneously.

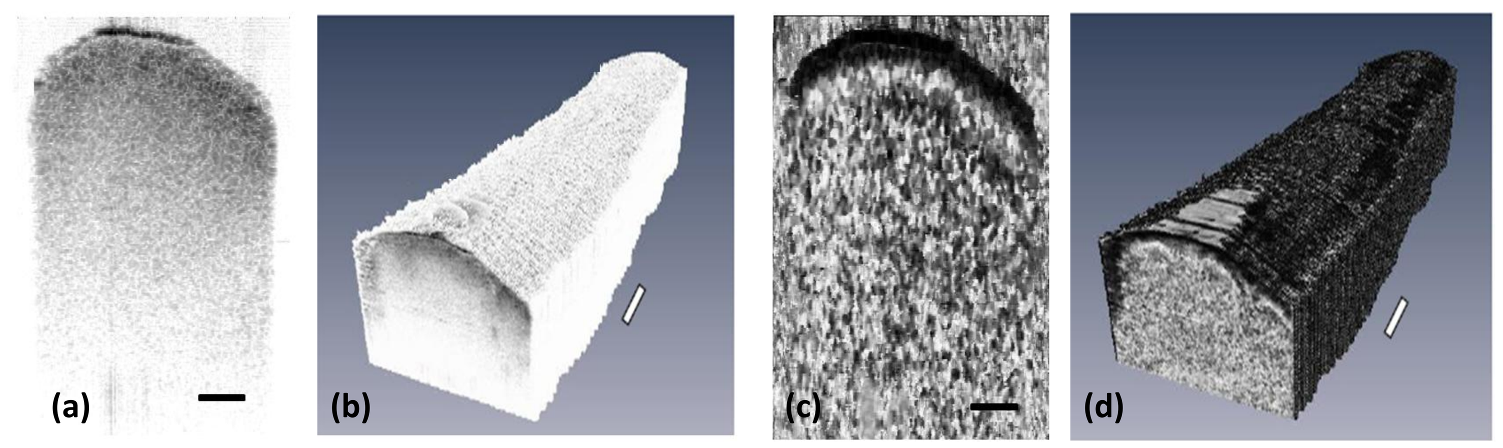

Figure 2. (a,c) 2D OCT and PS-OCT images. Bar: 200-um (b,d) 3D OCT and PS-OCT reconstructions from 2D images. Bar: 500-um

1. EPINEURIUM THICKNESS

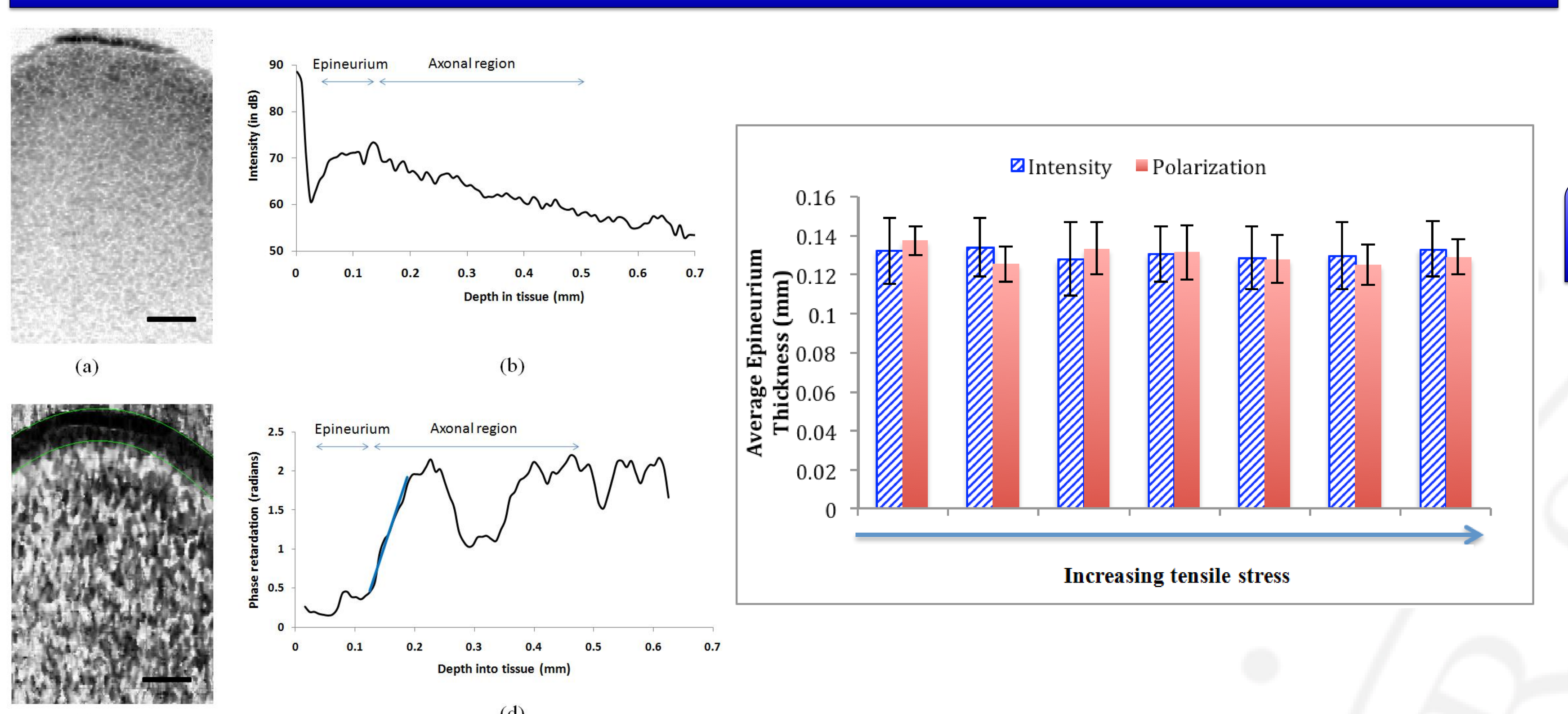

Figure 3. *Left.* (a,c) 2D OCT and PS-OCT images. Bar: 200-um (b,d) Intensity and phase retardation vs. depth into tissue. Epineurium regions denoted on the respective plots. *Right.* Bar chart demonstrating no change in epineurium thickness as the sciatic nerve is stretched and agreement between OCT and PS-OCT measurements

2. AVERAGE BIREFRINGENCE

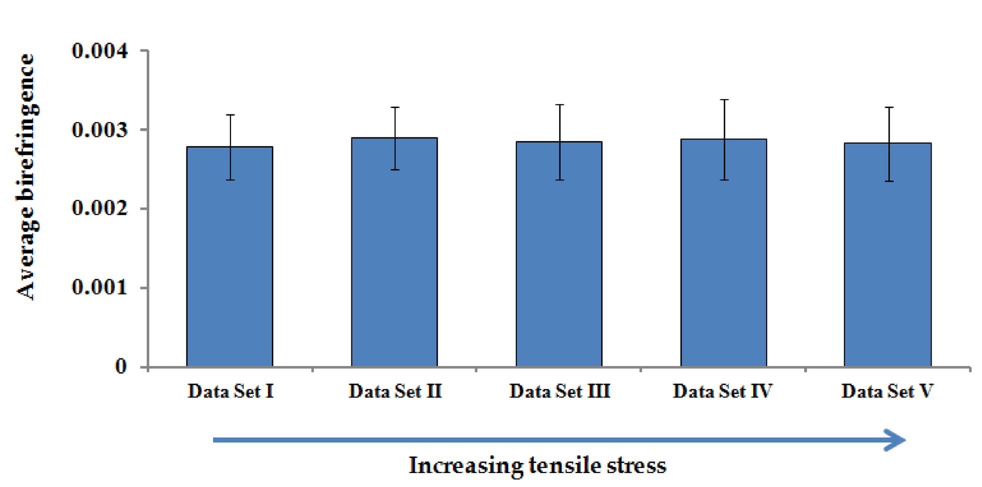

Figure 4. Bar chart demonstrating no change in average birefringence of the nerve as the sciatic nerve is stretched.

3. OPTICAL FEATURES

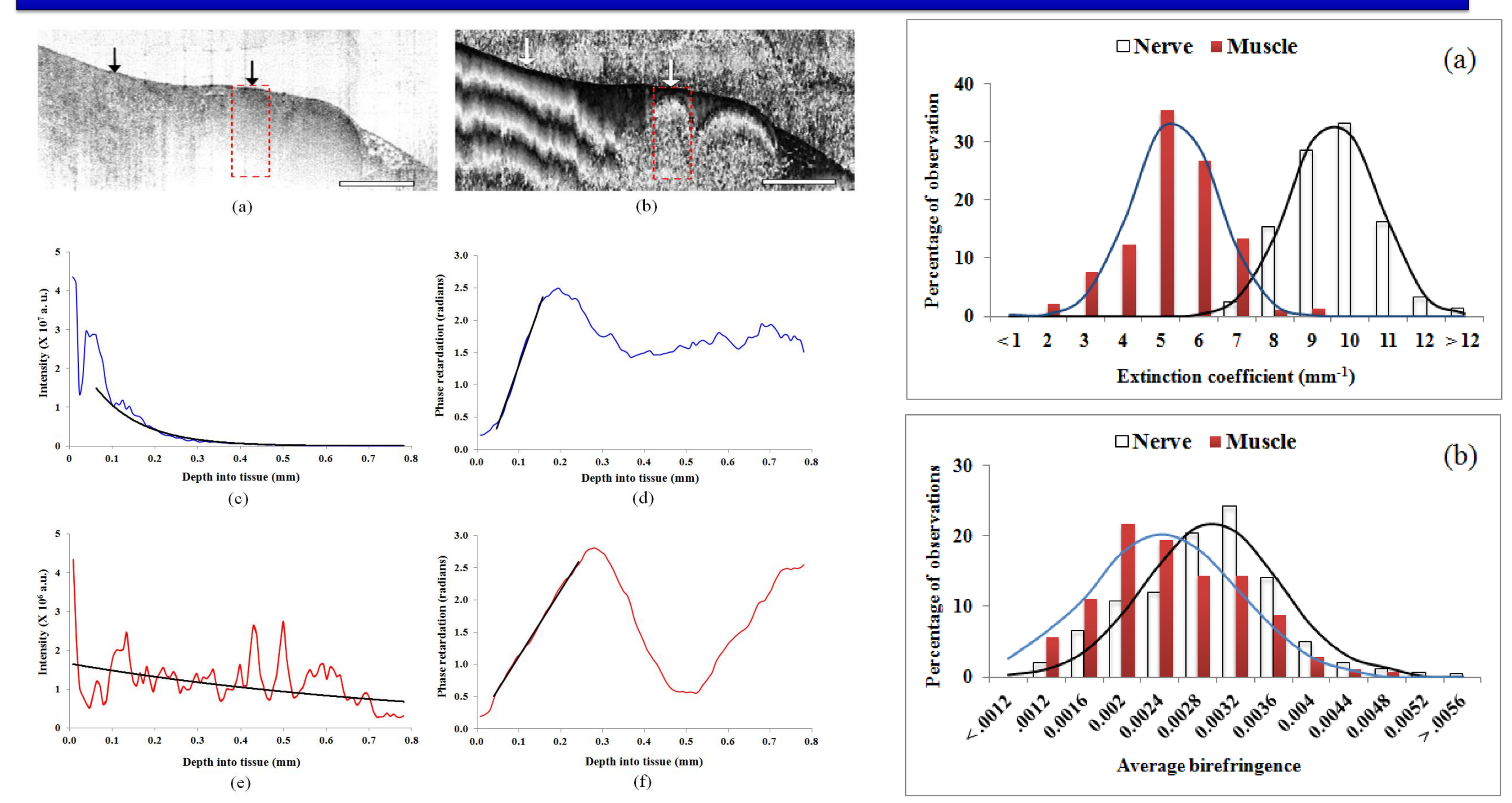

Figure 5. *Left.* (a,b) 2D *in vivo* OCT and PS-OCT images of the sciatic nerve surrounded by muscle tissue. Plots depict intensity decay vs. depth into tissue for nerve (c) and muscle tissue(e) and phase retardation vs. depth into tissue for nerve (d) and muscle tissue (f). *Right.* Histograms of the distribution of extinction coefficient (top) and birefringence (bottom) of nerve and muscle tissue.

4. FONTANA'S BANDS

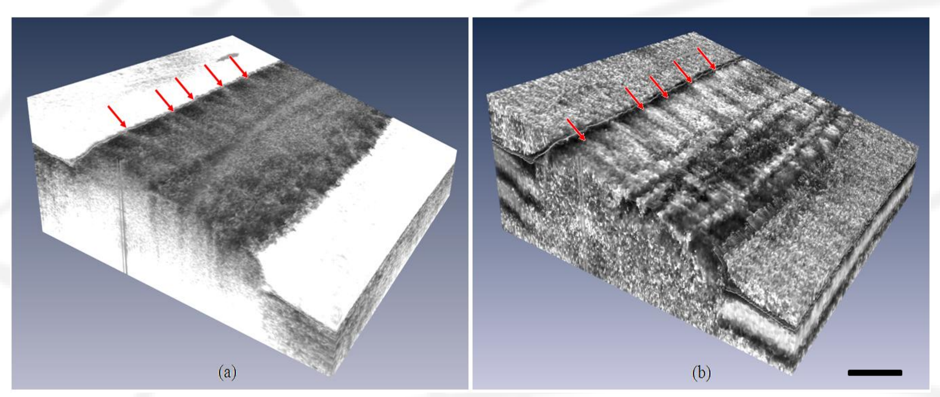

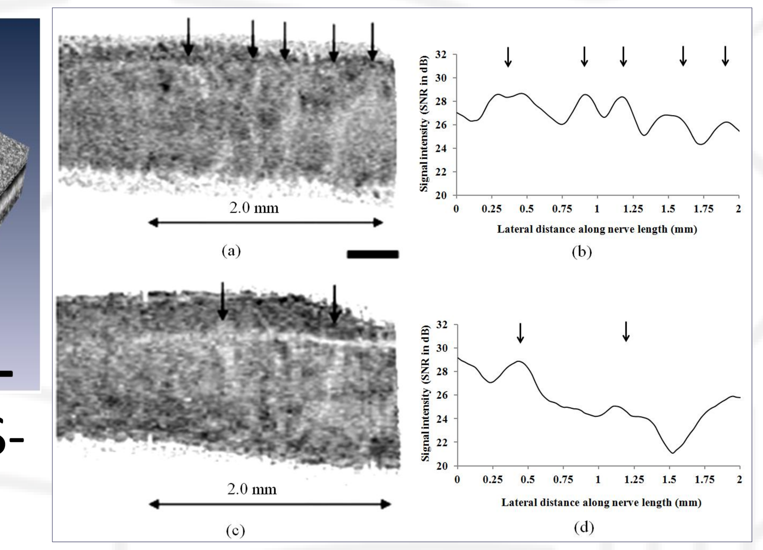

Figure 6. *Left. In vivo* OCT (a) and PS-OCT (b) 3D reconstructions of the sciatic nerve surrounded by muscle. Red arrows point to visible Fontana's bands. *Right.* Slices through a OCT 3D reconstruction showing the visibility of Fontana's bands for an un-stretched (a) and stretched (b) nerve. Corresponding plots of intensity along the axis of the nerve confirm the presence of the bands for an un-stretched (b) and stretched (d) nerve.

CONCLUSION

We successfully extracted important structural and optical features of the nerve and surrounding muscle tissue using multi-functional spectral-domain OCT. This serves as the groundwork for studying nerve injury in the future, as we have structurally and optically characterized healthy rat sciatic nerve. **Support for this work was provided by NSF IGERT: Video Bioinformatics Grant DGE 0903667.**